Comparative Biochemistry and Physiology, Part C 162 (2014) 51–61

Contents lists available at ScienceDirect

Comparative Biochemistry and Physiology, Part C

journal homepage: www.elsevier.com/locate/cbpc

Physiological hepatic response to zinc oxide nanoparticle exposure in the white sucker, *Catostomus commersonii*

Christopher Anthony Dieni *, Neal Ingraham Callaghan, Patrick Thomas Gormley, Kathryn Marie Alison Butler, Tyson James MacCormack

Department of Chemistry and Biochemistry, Mount Allison University, Barclay Chemistry Building, 63C York Street, Sackville, New Brunswick E4L 1G8, Canada

ARTICLE INFO

Article history:
Received 20 January 2014
Received in revised form 21 March 2014
Accepted 21 March 2014
Available online 3 April 2014

Keywords:
Assay validation
Fish
Liver response
Nanotoxicity
Oxidative stress
Zinc oxide nanoparticles

ABSTRACT

Liver toxicity of commercially relevant zinc oxide nanoparticles (nZnO) was assessed in a benthic freshwater cypriniform, the white sucker (*Catostomus commersonii*). Exposure to nZnO caused several changes in levels of liver enzyme activity, antioxidants, and lipid peroxidation end products consistent with an oxidative stress response. Aconitase activity decreased by ~65% but tended to be restored to original levels upon supplementation with Fe^{2+}, indicating oxidative inactivation of the 4Fe–4S cluster. Furthermore, glucose-6-phosphate dehydrogenase activity decreased by ~29%, and glutathione levels increased by ~56%. Taken together, these suggest that nZnO induces hepatic physiological stress. Each assay was then validated by using a single liver homogenate or plasma sample that was partitioned and treated with nZnO or Zn^{2+}, the breakdown product of nZnO. It was found that Zn^{2+}, but not nZnO, increased detected glutathione reductase activity by ~14% and decreased detected malondialdehyde by ~39%. This indicates that if appreciable nZnO dissolution occurs in liver samples during processing and assay, it may skew results, with implications not only for this study, but also for a wide range of nanotoxicology studies focusing on nZnO. Finally, in vitro incubations of cell-free rat blood plasma with nZnO failed to generate any significant increase in malondialdehyde or protein carbonyl levels, or any significant decrease in ferric reducing ability of plasma. This suggests that at the level tested, any oxidative stress caused by nZnO is the result of a coordinated physiological response by the liver.

1. Introduction

The use of engineered nanomaterials (ENMs), part of the broad spectrum of our modern-day array of nanotechnological tools, has increased drastically over recent years (Aitken et al., 2006; Westerhoff and Nowack, 2012). ENMs are now deliberately synthesized for use as biosensors and assay tools (Wang, 2005), as delivery vehicles for a diverse number of therapeutics (Nie, 2010), and in cosmetic products such as sunscreens (Mu and Sprando, 2010); they are also created incidentally as by-products of manufacturing processes (Park et al., 2011). Due to their expansive use, ENMs are being released into the environment (particularly aquatic environments) and are coming into contact with the organisms present; the incidence of exposure has now outpaced our understanding of the potential risks and hazards of ENMs as a whole (Handy et al., 2008B).

ENMs can exert their toxicity via an array of mechanisms, with two broad "types" of in vivo mechanisms being of particular interest. One type of mechanism is through direct physical contact with biological macromolecules. Nanoparticle–protein interactions are commonplace (Lynch and Dawson, 2008) and it is now well-established that a "protein corona" forms around ENMs within biological media (Rahman et al., 2013); we have recently demonstrated that these nanoparticle–protein interactions can disrupt the ligand binding properties of proteins (Dieni et al., 2013). From the perspective of systemic toxicity, altering protein–ligand interactions can have widespread, deleterious effects on an organism's global metabolism including lipid transport, drug distribution, and ion homeostasis (e.g. Cedervall et al., 2012). A second type mechanism of ENM toxicity is the generation of reactive oxygen species (ROS; and alternatively reactive nitrogen species) through a number of pathways, including 1) the adsorption of redox-cycling biomolecules to the ENM surface and 2) the formation of active electron configurations by virtue of imperfections in the ENM's nanostructure (Nel et al., 2006; Xia et al., 2008; Rasmussen et al., 2010). Typically, it has been reported in these studies that superoxide ($O_2^{\bullet -}$) can be formed in vivo from the interaction of molecular oxygen (O_2) with ENM-activated electron configurations. Superoxide can then enzymatically or non-enzymatically dismutate to hydrogen peroxide (H_2O_2); if levels of peroxide are high enough, or are localized in biological compartments where disproportionation via catalase cannot occur rapidly, peroxide can undergo a Fenton reaction with redox-cycling metals (e.g. Fe^{2+}) to produce the much more reactive peroxyl (•OOH)

* Corresponding author. Tel.: +1 506 364 2588; fax: +1 506 364 2455.
E-mail address: cdieni@mta.ca (C.A. Dieni).

http://dx.doi.org/10.1016/j.cbpc.2014.03.009
1532-0456/

or hydroxyl (•OH) radicals (Nel et al., 2006; Prousek, 2007; Luna-Velasco et al., 2011). These highly-reactive radicals can then interact with numerous extracellular and intracellular components including metabolites, proteins, lipids, and DNA, damaging them and propagating reactive species even further. "Oxidative stress" is a term used to define when a threshold has been crossed where ROS levels and ROS-induced damage accumulate to a point where endogenous antioxidant defenses or repair systems can no longer keep pace (Finkel and Holbrook, 2000).

Using a variety of cell and animal models, the argument for the toxic potential of zinc oxide nanoparticles (nZnO) is gaining increasing support (Xia et al., 2008; Bai et al., 2010; Cho et al., 2011; Shaw and Handy, 2011; Guo et al., 2013). However, its potential importance cannot be overlooked; nZnO has been used as therapeutic in preliminary studies using streptozotocin-induced diabetic rats (Umrani and Paknikar, 2014), and it is used alongside titanium dioxide (TiO_2) nanoparticles in sunscreens for their diffractive effects on UV sunlight (Mu and Sprando, 2010). Given these beneficial nanotechnological applications, nZnO continues to be liberally used with lesser regard for its release into the environment and possible consequences. TiO_2, used alongside nZnO in sunscreens, is now persistently detectable in beach waters (Botta et al., 2011); it is not unreasonable to assume that nZnO is, or will soon become, equally prevalent in the environment. With this increased dependency on its purported benefits, and its resulting increased environmental prevalence, assessing the toxic potential of nZnO at low aquatic levels is now even more important than in times prior to the advent of widespread ENM use.

In this study, we investigate the effects of nZnO exposure in the liver of a freshwater fish, the white sucker (*Catostomus commersonii*). We examine liver biomarkers of oxidative stress and antioxidant responses, and compare these findings to the in vitro effects of nZnO in a complex biological medium, blood plasma. We demonstrate here that whole animal EMN exposure induces a hepatic response consistent with oxidative stress, but that this response requires a living unit (e.g. at the very least, a living cell) and does not appear to be due to direct effects of ENMs on plasma constituents. Our results also reinforce the need to validate all assays, in order to accurately account for any bias induced by the presence of ENMs or ENM degradation products.

2. Material and methods

2.1. Material

2.1.1. Reagents and enzymes

Reagents and enzymes purchased from Sigma-Aldrich Co. (St Louis, MO, USA) include the following: adenosine triphosphate (ATP), bovine serum albumin (BSA), 2,4-dinitrophenylhydrazine (DNPH), ethanol, ethyl acetate, ethylenediaminetetraacetic acid (EDTA) glucose-6-phosphate (G6P), glycine buffer, guanidine hydrochloride (GdnHCl), isocitrate dehydrogenase (IDH), nicotinamide adenine dinucleotide (reduced; NADH), sodium bicarbonate ($NaHCO_3$), sodium chloride (NaCl), sodium phosphate, and 2,4,6-tris(2-pyridyl)-s-triazine (TPTZ). Reagents and enzymes purchased from BioShop Canada Inc. (Burlington, ON, Canada) include: β-glycerophosphate, ethyleneglycoltetraacetic acid (EGTA), hydrogen peroxide (H_2O_2), glutathione (oxidized; GSSG), nicotinamide adenine dinucleotide phosphate (both oxidized and reduced forms; $NADP^+$ and NADPH), phenylmethylsulfonyl fluoride (PMSF), tribasic potassium citrate, and trichloroacetic acid (TCA). Calcium chloride ($CaCl_2$) was purchased from Anachemia/VWR (Radnor, PA, USA), ferrous ammonium sulfate was purchased from Fisher Scientific (Waltham, MA, USA), ferric chloride ($FeCl_3$) and magnesium chloride ($MgCl_2$) were purchased from ACP Chemicals Inc. (Montreal, QC, Canada), and potassium chloride (KCl) was purchased from Caledon Laboratories Ltd. (Georgetown, ON, Canada). Sprague Dawley rat plasma with sodium citrate anticoagulant was purchased from Innovative Research (Novi, MI, USA) distributed by Cedarlane Labs (Burlington, ON, Canada). All other reagents were obtained in kit format and are identified in the description of their individual assays.

2.1.2. Engineered nanomaterials

The ENMs used in this study were spherical nZnO with an unknown surface functionalization, an advertised diameter of 25 nm, and a ζ potential of +23.5 mV (Nanocomposix, San Diego, CA, USA). This specific nZnO formulation is part of a library of materials curated by the supplier which represent ENMs produced in large quantities for use in consumer products and is therefore considered environmentally-relevant. nZnO are shipped in solid (powder) format, and were stored in the dark at 4 °C until use. A fresh stock solution of 1 mg/mL was made for each trial; 30 mg of nZnO was suspended in 30 mL of MilliQ water and dispersed using a wand-type sonicator immediately prior to use.

Characterization data, provided by the supplier, is presented in Table 1. Supplemental on-site dynamic light scattering analysis was undertaken using a Zetasizer Nano ZS (Malvern Instruments, Worcestershire, UK). Fresh nZnO stock suspensions (prepared as described above) were diluted to 100 mg/L in MilliQ water and sonicated for 30 s using a wand-type sonicator immediately prior to analysis. Hydrodynamic diameter and ζ potential were assessed according to the recommendations of the instrument manufacturer, and were found to compare well to supplier data (331.9 nm hydrodynamic diameter, +21.1 mV ζ potential, 0.351 polydispersity index). Accurate characterization of hydrodynamic diameter via nanoparticle tracking analysis (Nanosight LM10-HS) was not possible due to the heterogeneous nature of the nZnO dispersion. Primary particle diameter was qualitatively confirmed by drying down nZnO suspensions onto polished graphite specimen supports and sputter coating with ca. 5 nm gold using a Hummer 6.2 sputtering system (Anatech USA, Union City, CA, USA). Preparations were examined using a JEOL JSM-5600 scanning electron microscope (JEOL USA, Inc., Peabody, MA, USA) operating at 10 kV and 8 mm working distance (Fig. 1).

2.2. Experimental protocols

2.2.1. Fish exposures to nZnO

Wild male and female white suckers (*C. commersonii*; body mass 217 ± 52 g) were collected from Silver Lake (Sackville, NB, Canada) during the summer of 2012 (May–August). Fish were held in tanks of circulating freshwater (10–12 °C) for a minimum of 2 weeks before experimentation. All procedures were performed with the approval of the Mount Allison University Animal Care Committee. Fish were not fed the day before or during an experiment.

A 45 L chest cooler (Coleman, Wichita, KS, USA) was modified to be used as an experimental tank to hold the fish during exposure to nZnO or control conditions. Small diameter, stainless steel piping was fitted around the internal perimeter of the tank and connected to an external, refrigerated circulator (VWR, Radnor, PA, USA) in order to maintain a water temperature of approximately 10 °C. An aeration stone was

Table 1
Characterization data of 25 nm zinc oxide nanoparticles (nZnO), comparing data provided by the manufacturer (Nanocomposix, San Diego, CA, USA) and additional on-site characterization using a Zetasizer Nano ZS (Malvern Instruments, Worcestershire, UK). ND = not determined.

Characteristic	Manufacturer's data	On-site characterization
Diameter (nm)	25.1	ND
Coefficient of variation (%)	42.8	ND
First standard deviation (nm)	10.8	ND
Water miscible	Yes	Yes
Hydrodynamic diameter (nm)	284.3	331.9
Zeta (ζ) potential (mV)	+28.1	+21.1
Polydispersity index	0.339	0.351

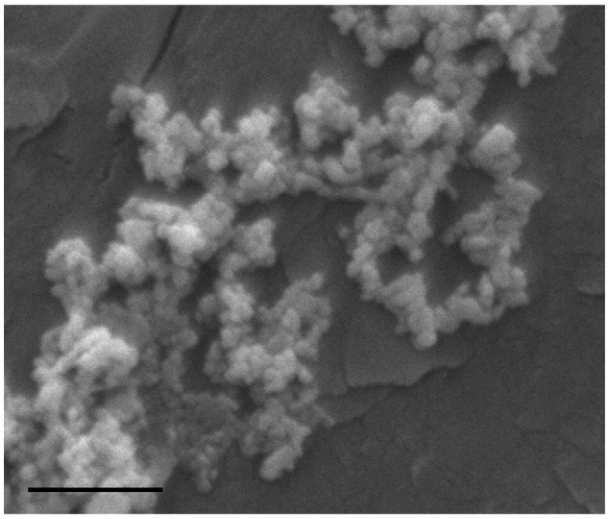

Fig. 1. Scanning electron micrograph of dried nZnO. Scale bar = 500 nm.

used to ensure consistent levels of dissolved oxygen in the tank and a circulation pump ensured that the oxygen and nZnO were evenly dispersed within the system. During the experiment, fish were placed within a perforated PVC pipe (3.5″ diameter) submerged in the experimental tank. The pipe allowed for horizontal movement, but restricted the fish from vertical movement or turning around. The experimental tank was filled with 30 L of dechlorinated freshwater for each trial that was either untreated or contained a final concentration of 1 mg/L nZnO. A 1 mg/mL nZnO stock solution was prepared fresh for each exposure and sonicated just prior to addition. Fish were allowed to acclimate to the experimental system for approximately 15.5 h before treatment. Fish were exposed to 1 mg/L nZnO for 29.5 h. Ammonia, nitrate, and nitrite levels were determined using a Nutrafin® Ammonia Test kit, Nitrate Test kit, and Nitrite Test kit (Hagen, Masfield, MA, USA), respectively, and were well within acceptable limits at the end of each experiment (data not shown).

At the conclusion of this 45 hour period, fish were killed by MS-222 overdose and then pithed before tissue sampling. Blood was collected from the caudal vein with a heparinized syringe, immediately centrifuged at 1700 *g* for 4 min at 13 °C, and plasma was removed and flash-frozen in liquid nitrogen. The liver and a number of other tissues were sampled, immediately flash-frozen in liquid nitrogen, and stored at −80 °C until further analysis. Seven white suckers were exposed to 1 mg/L nZnO, and another 7 were kept under control conditions.

2.2.2. In vitro incubations of rat plasma and nZnO

A commercial preparation of rat (*Rattus norvegicus*) plasma (purchased as a 500 mL volume of pooled plasma derived from the whole blood of on-average 125–250 healthy rats) was aliquoted into 15 mL conical tubes and warmed to 37 °C. Three different in vitro conditions were established, each consisting of a 9:1 ratio of plasma: treatment in a 10 mL final volume. Treatments were the following: i) saline (0.9% NaCl; a negative control); ii) 10% H_2O_2 (final concentration 1%; a positive control), and; iii) 10 mg/L of freshly-sonicated nZnO suspended in saline (final concentration of 1 mg/L; the equivalent concentration to which white suckers were exposed). Immediately upon addition of the treatment (saline, 10% H_2O_2, or 10 mg/L nZnO) to plasma, each sample was thoroughly mixed by inversion, and half of the total volume (~5 mL) was flash-frozen in liquid nitrogen and stored at −80 °C; this was our "0 h" or "before incubation" time-point. The remaining volumes were incubated on a laboratory rotator for 48 h at 37 °C. Certain H_2O_2 positive controls (i.e. malondialdehyde and protein carbonyl groups) were incubated for 24 h because linear changes from H_2O_2-mediated damage were observed during that time-frame, based on optimization experiments. At the end of these incubations (our "after incubation" point), the remaining volume of plasma was flash frozen in liquid nitrogen and stored at −80 °C until assay. This procedure, in its entirety (from treatment preparation to assay), was repeated at least twice more, to provide a minimum of 3 individual replicates.

2.3. Assay methods

2.3.1. Processing of liver samples for enzyme and metabolite analysis

Liver samples were removed from −80 °C storage and kept in liquid nitrogen until immediately prior to homogenizing. Each individual liver sample (on average ~57 ± 23 mg) was quickly weighed on an analytical balance and suspended in a volume of homogenizing buffer (50 mM sodium phosphate, 5 mM EDTA, 5 mM EGTA, 30 mM β-glycerophosphate, pH 7.2) that was 5 times the mass of the liver sample. A volume of PMSF stock solution (200 mM PMSF in ethanol) that was 0.5% of the volume of homogenizing buffer used was also added immediately before homogenization, for a final concentration of 1 mM PMSF. Liver samples were then homogenized on ice, to preserve enzyme activity, using a Polytron® PT 10-35 GT laboratory homogenizer (Kinematica, Lucerne, Switzerland). The homogenizer was run at full power for 10 second bursts, allowing for 10 second cooling intervals between bursts, until the liver sample was completely homogenized. Homogenates were transferred to microtubes and centrifuged at 10,000 *g* for 10 min at 4 °C. Supernatants were collected and kept on ice, whereas pellets were discarded.

A TCA stock solution (50% w/v TCA) was then added to an aliquot of supernatant in a 1:9 ratio of TCA:supernatant (final TCA concentration in this mixture was thus 5% w/v), and thoroughly vortexed. TCA-supernatant mixtures were centrifuged once again at 10,000 *g* for 10 min at 4 °C. The TCA-clarified supernatants were collected (pellets were discarded) and stored at −80 °C until immediately prior to glutathione assay.

2.3.2. Malondialdehyde assay

Levels of malondialdehyde (MDA), the end-product of lipid peroxidation, were assayed in undiluted liver supernatants and in vitro rat plasma incubations using the colorimetric endpoint assay of the BIOXYTECH® MDA-586™ assay kit (Percipio Biosciences, Berlingame, CA, USA), according to the manufacturer's instructions, but using one-half of the volumes directed. Briefly, 100 μL of undiluted liver supernatant or rat plasma incubations was transferred to fresh microtubes, to which 5 μL of probucol was added, and this mixture was thoroughly vortexed. Diluted reagent R1 (320 μL; a 3:1 ratio of stock reagent R1: methanol) was then added, and the mixture was vortexed again. Reagent R2 (75 μL) was added, and the mixture was vortexed again. Microtubes were then incubated on a laboratory heating block at 45 °C for 1 h, after which they were centrifuged at 10,000 *g* for 10 min, at 4 °C. Three aliquots of 100 μL for each sample were transferred to wells of clear polystyrene 96-well microplates (Greiner Bio-One, Monroe, NC, USA; Cat. No. 655101) for triplicate readings of each sample, and absorbance at 586 nm was measured in a SpectraMax® 190 Absorbance Microplate Reader (Molecular Devices, Sunnyvale, CA, USA). These triplicate readings were then averaged to provide a single absorbance for each replicate. Concentrations of unknown MDA levels were determined by comparison to a linear standard curve of tetramethoxypropane (TMOP) ranging from 6.7 to 50 μM TMOP. MDA levels were represented as a mole quantity of MDA normalized to total protein in liver supernatants (e.g. nmol/mg), or as relative levels within the uniform commercial plasma preparation.

2.3.3. Liver protein assay

Protein concentrations in liver supernatants were assayed using the colorimetric endpoint assay of the bicinchoninic acid (BCA) kit for protein determination (Sigma-Aldrich, St. Louis, MO, USA), according

to the manufacturer's instructions for microplate format. Briefly, a BCA working reagent was prepared by mixing reagent A and reagent B in a 50:1 ratio of reagent A:reagent B. Liver supernatants were diluted 1 in 10 with homogenizing buffer so that they fell within the linear range of the assay. In a clear 96-well microplate, 25 μL of diluted liver supernatant was added to 200 μL BCA working reagent. Microplates were covered with parafilm and incubated at 37 °C for 30 min. Following incubation, absorbance at 562 nm was measured in the microplate reader. Concentrations of unknown protein levels were determined by comparison to a linear standard curve of bovine serum albumin (BSA) ranging from 0.21 to 1 mg/mL BSA.

2.3.4. Liver enzyme assays

Three liver enzymes were assayed to investigate specific aspects of a possible oxidative stress response: glucose-6-phosphate dehydrogenase (G6PDH; EC 1.1.1.49), glutathione reductase (GR; EC 1.8.1.7), and aconitase (EC 4.2.1.3). These enzymes were assayed using microplate-format colorimetric kinetic enzyme assays in clear 96-well microplates with a 200 μL final assay volume. Final assay conditions used for G6PDH were: 50 mM sodium phosphate, pH 7.2, 10 mM $MgCl_2$, 5 mM G6P, and 500 μM $NADP^+$. Final assay conditions used for GR were: 50 mM sodium phosphate, 0.5% TCA, pH 6.5, 5 mM oxidized glutathione (GSSG), and 200 μM NADPH. Final assay conditions used for aconitase were: 50 mM sodium phosphate, pH 7.2, 1 mM $MgCl_2$, 2 mM Mg^{2+}-citrate (from a stock solution of 20 mM $MgCl_2$ and 20 mM tribasic potassium citrate), 500 mU IDH, an optional 200 μM ferrous ammonium sulfate (for reactivating inactivated aconitase), and 500 μM $NADP^+$. For each enzyme, a "blank" assay was also included which omitted each enzyme's more specific substrate and replaced its volume with MilliQ water; glucose-6-phosphate was omitted for G6PDH blanks, GSSG was omitted for GR blanks, and citrate was omitted for aconitase blanks. This allowed for a determination of any appreciable rate of off-target consumption or production of NADPH caused by other endogenous components of liver supernatants (blank rate), and the blank rate of reaction was then subtracted from the rate of reaction in presence of the aforementioned substrates.

Liver supernatants were first diluted using homogenizing buffer, so that a linear rate of reaction could be followed over several minutes by using 10 μL of diluted liver supernatant within the 200 μL final assay volume. For GR, this necessitated a 1 in 5 dilution of liver supernatant in homogenizing buffer; for G6PDH and aconitase, a 1 in 10 dilution was needed. Reactions were initiated by the addition of the appropriate NADP(H) nucleotide (either $NADP^+$ for G6PDH and aconitase, or NADPH for GR). Changes in absorbance at 340 nm caused by the consumption (by GR) or production (by G6PDH and aconitase) of NADPH were followed in the microplate reader, incubated at 37 °C and taking absorbance readings at 10–15 s intervals. Initial rates of reaction were calculated from the linear portions of the curve. Changes in absorbance were converted into changes in concentration by using a molar absorptivity (ε) of 6.22 mM^{-1} cm^{-1} for NADPH, and the measured path length (l) of 200 μL of liquid in a 96-well microplate was approximately 1 cm. Activities were represented as changes in a mole quantity over time, normalized to total protein in liver supernatants (e.g. pmol/min/mg).

2.3.5. Liver glutathione assay

Levels of total glutathione were assayed in TCA-clarified liver supernatants using the colorimetric kinetic assay of the OxiSelect™ Total Glutathione (GSSG/GSH) Assay Kit, (Cell Biolabs, San Diego, CA, USA), according to the manufacturer's instructions, except that TCA was used in all instances where metaphosphoric acid (MPA) would have otherwise been used. Briefly, TCA-clarified liver supernatants were mixed with a stock solution of ethanol, triethanolamine, and MilliQ water (ETW; 25% ethanol, 25% triethanolamine, 50% MilliQ water) in a 9:1 ratio of supernatant:ETW. This supernatant-ETW mixture was then serially diluted to a factor of 10^{-3} in dilution buffer (50 mM sodium phosphate, 0.5% TCA, pH 6.5). Diluted supernatant was transferred to wells of clear 96-well microplates, and added to NADPH and GR that had been provided with the kit and prepared according to instructions. Assays were initiated with the addition of "1× chromogen" (the exact nature of this chromogen or oxidizing agent is not described in the kit manual, however, it was prepared according to instructions) and changes in absorbance at 340 nm caused by the consumption of NADPH were followed in the microplate reader, incubated at 37 °C and taking absorbance readings at 10–15 second intervals. Initial rates of reaction were calculated from the linear portions of the curve. Concentrations of glutathione in unknown samples were determined by comparison to a linear standard curve of GSSG (provided with the kit) ranging from 0 to 500 nM. Glutathione levels were represented as a mole quantity of glutathione normalized to total protein in liver supernatants (e.g. nmol/mg).

2.3.6. Validation of liver-based assays

Nanoparticles have been shown to interfere with a number of assay methods by interactions with the specific analytes to be detected, as well as coupling enzymes and coupling/detection substrates (e.g. Handy et al., 2012; MacCormack et al., 2012; Ong et al., 2014). To ensure that data obtained in this study were the result of in vivo changes as a physiological response to nanotoxicants, and not an effect of nZnO or Zn^{2+} interfering with assay methods or otherwise creating an assay bias in vitro, a series of validations were carried out.

Two liver samples from fish not exposed to nZnO were homogenized together (in order to provide a large-enough working volume of a uniform homogenate) in homogenizing buffer and PMSF as described above. Prior to centrifugation, this homogenate was evenly partitioned into 3 parts. To each of these 3 partitions was added one of 3 types of treatments, either 1) MilliQ water, 2) 10 mg/L $ZnCl_2$, or 3) 10 mg/L nZnO (serially diluted from a freshly-prepared and sonicated 1 mg/mL nZnO stock), in a 1:9 ratio of treatment:liver homogenate. This resulted in liver homogenates "spiked" to final concentrations of 1 mg/L Zn^{2+} or nZnO, the final concentration of nZnO to which fish were exposed in tanks. The 3 treatments of homogenates were then centrifuged as described above, with supernatant collected, and part of that supernatant clarified with TCA. Assays for MDA, protein concentration G6PDH, GR, aconitase, and glutathione were carried out in triplicate as before, and resulting values from each of the 3 treatments of homogenates were compared.

No separate validation steps were needed with our in vitro rat plasma-nZnO incubations. This was due to the simple fact that samples of these preparations were collected immediately upon the introduction of nZnO to the plasma ($t = 0$ h). If the nZnO interfered with any assays used for the rat plasma, this would have been readily apparent from any differences between the saline control and the 1 mg/L nZnO treatment at $t = 0$ h.

2.3.7. Protein carbonyl group assay

Levels of protein carbonyl groups, an end-product of protein oxidative damage, were determined in in vitro rat plasma incubations via an endpoint spectrophotometeric analysis. For each condition of the in vitro incubations, two plasma samples (100 μL; one designated "test" and one designated "blank") were added to a TCA solution (10% w/v TCA) in clean microtubes at a 1:6 ratio of plasma:TCA, and mixed thoroughly. These were then centrifuged at 13,000 *g* for 5 min at room temperature. Supernatants were discarded, and pellets were resuspended with either 0.4 mL of a DNPH solution (10 mM DNPH dissolved in 2 M HCl) for test pellets, or 0.4 mL of 2 M HCl for blank pellets. These were incubated for 1 h at room temperature, followed by centrifugation at 13,000 *g* for 5 min at room temperature. Supernatants were again discarded, and pellets (both test and blank) were washed 3× with a 1:1 solution of ethanol:ethyl acetate (0.6 mL). Pellets were resuspended in 0.6 mL 6 M GdnHCl, and immediately centrifuged at 13,000 *g* for 5 min at room temperature. 200 μL of each supernatant

was transferred to wells of clear 96-well microplates, and the absorbance was measured at 370 nm. For each incubation sample, absorbance values of "blank" assays (pellets resuspended in 2 M HCl) were subtracted from "test" assays (pellets resuspended in 10 mM DNPH, 2 M HCl) to provide a corrected absorbance. Levels of protein carbonyl groups were represented as relative levels within the uniform commercial plasma preparation.

2.3.8. Ferric reducing ability of plasma assay

Ferric reducing ability of plasma (FRAP), an indicator of antioxidant potential in complex biological media (particularly in blood plasma), was assessed in in vitro rat plasma incubations via an endpoint spectrophotometeric analysis. FRAP "test" and "blank" reagent working solutions were prepared by combining TPTZ stock solution (10 mM TPTZ in 40 mM HCl), $FeCl_3$ stock solution (20 mM $FeCl_3$) or water, and sodium acetate stock solution (0.3 M sodium acetate, pH 3.6) in a 1:1:10 ratio of TPTZ:$FeCl_3$:acetate for the "test" working solution, and 1:1:10 ratio of TPTZ:water:acetate for the "blank" working solution. 250 μL of either the test or blank solution was added to wells of clear 96-well microplates, and each of these wells was then supplemented with 35 μL MilliQ water. To the wells containing test or blank FRAP working reagent was finally added 25 μL of sample from in vitro rat plasma incubations, so as to test for the FRAP of each sample while accounting for any reduced Fe^{2+} already present in plasma. Microplates were incubated for 10 min at 37 °C, and the absorbance was measured at 595 nm. FRAP levels in rat plasma were determined by comparison to a linear standard curve of Fe^{2+} from ferrous ammonium sulfate ranging from 0.2 to 1 mM; these were represented as relative levels within the uniform commercial plasma preparation.

2.4. Data analysis

Statistics were analyzed using SPSS® Statistics 21 (IBM, Armonk, NY, USA) and Prism 4 (GraphPad, La Jolla, CA, USA). All data were initially assessed for normality via the Shapiro–Wilk test (and confirmed visually by histograms and Q–Q plot graphical tests) by analyzing all cases simultaneously (i.e. not splitting groups between different fish treatments, validation treatments, or plasma treatments); data that were found to be normally distributed were then tested for homogeneity of variance by Levene's test, with each independent variable (i.e. control vs nZnO-exposed fish, "spiked" liver homogenates, and treated plasma incubations) now separated into different groups to assess the variance of each.

G6PDH activity, GR activity, glutathione levels and MDA levels consisted of data with one independent variable separated into two groups (i.e. control vs nZnO-exposed fish). Based on results for normality and homogeneity of variance tests, each individual parameter was then assessed by 1) unpaired t-tests, where equal variances were respectfully assumed or not assumed as per the earlier results of Levene's test, or 2) by the nonparametric independent-samples Mann–Whitney U test. Data for aconitase activities consisted of two independent variables separated into two groups (i.e. liver homogenates from control vs nZnO-exposed fish, where aconitase was assayed unsupplemented vs Fe^{2+}-supplemented aconitase assays). With both assumptions for normality and homogeneity of variance tested and fulfilled as described above, effects on aconitase activities were then assessed by two-way ANOVA followed by Bonferroni post-tests; statistical differences between specific groups (e.g. unsupplemented aconitase activities from control fish vs. Fe^{2+}-supplemented activities from control fish, etc.) were then determined by post-hoc unpaired t-tests, where equal variances were assumed as per the earlier results of Levene's test.

Data for the aforementioned enzyme activities, metabolite levels, and protein levels in liver homogenates "spiked" with MilliQ water, $ZnCl_2$, and nZnO (i.e. assay validations) consisted of a single independent variable separated into three groups. Based on results for normality and homogeneity of variance, statistically significant differences were analyzed with either 1) one-way ANOVA followed by Tukey's multiple comparison tests, or 2) nonparametric Kruskal–Wallis tests. By contrast, aconitase activities in liver assay validations – with both assumptions once again met – were assessed by two-way ANOVA followed by Bonferroni post-tests.

Data for levels of MDA, protein carbonyls, and FRAP in rat plasma incubations consisted of repeated measures of values for two independent variables separated into two groups (i.e. saline control vs nZnO-treated plasma, before vs after incubation). Based on normality and homogeneity of variance, statistically significant differences were analyzed with 1) paired t-tests (for a given treatment before vs after incubation), 2) unpaired t-tests assuming unequal variance (between different treatments), 3) nonparametric independent-samples Mann–Whitney U test, or 4) nonparametric Wilcoxon signed-rank tests, as each individual case dictated. H_2O_2 was used as a positive control primarily to establish the functionality of these assays for oxidative stress. We therefore opted to analyze our results on the basis of the two categorical variables (saline and nZnO exposure), hence H_2O_2 incubations were not included in a repeated measures ANOVA of three conditions; instead, differences between plasma-treated and H_2O_2-treated plasma samples before and after incubation were compared via the same four tests used to compare saline-treated and nZnO-treated plasma before and after incubation.

3. Results

3.1. Effects of acute exposure of live white suckers to 1 mg/L nZnO

All animals survived the 1 mg/L nZnO exposure and no overt morbidity was observed. Changes were observed in liver enzyme activities, levels of antioxidants, and markers of oxidative damage, overall indicative of oxidative stress in nZnO-exposed fish.

3.1.1. Liver enzyme activities

Liver G6PDH, GR, and aconitase were assayed from the crude supernatants of liver homogenates prepared from control fish and fish that were exposed to nZnO (Fig. 2). Statistically significant decreases were observed in the activities of G6PDH and aconitase, but not GR. G6PDH activity decreased by 29.2% as a result of nZnO exposure (Fig. 2A; $n = 7$ for both control and nZnO-exposed fish, $p = 0.014$ by unpaired t-test assuming unequal variance). GR activity was unchanged (Fig. 2B); this data was not normally distributed by the Shapiro–Wilk test ($p < 0.01$), but no significant differences were found in the distribution of data by the independent-samples Mann–Whitney U test. Aconitase activity displayed the sharpest decrease of the three enzymes assayed (Fig. 2C). Assessment by two-way ANOVA indicated that aconitase activities were significantly affected by both nZnO exposure ($p = 0.018$) and Fe^{2+} supplementation ($p = 0.027$), but that there was not a significant interaction ($p = 0.078$). A 65.1% decrease in activity was observed in fish exposed to nZnO when enzyme assays were unsupplemented ($n = 7$ control fish and 6 nZnO-exposed fish; $p < 0.001$ by post-hoc unpaired t-test assuming equal variance). When aconitase assays were supplemented with Fe^{2+} (in the form of ferrous ammonium sulfate), aconitase activity from control fish did not significantly increase compared to activity observed in unsupplemented assays; however, aconitase from nZnO-exposed fish significantly rose ($n = 7$ control fish and 5 nZnO-exposed fish, $p = 0.049$ by post-hoc unpaired t-test assuming equal variance), restored to an activity equivalent to that observed in control fish. This suggests that the drop in activity observed in nZnO-exposed fish is due to the oxidative inactivation of aconitase (Ott et al., 2007) via disruption of its labile 4Fe–4S cluster, and that replacement of the labile Fe^{2+} restores activity.

3.1.2. Liver MDA and total glutathione levels

Liver MDA levels were assayed from the crude supernatants of liver homogenates prepared from control fish and fish exposed to nZnO, whereas total glutathione levels were assayed from TCA-clarified

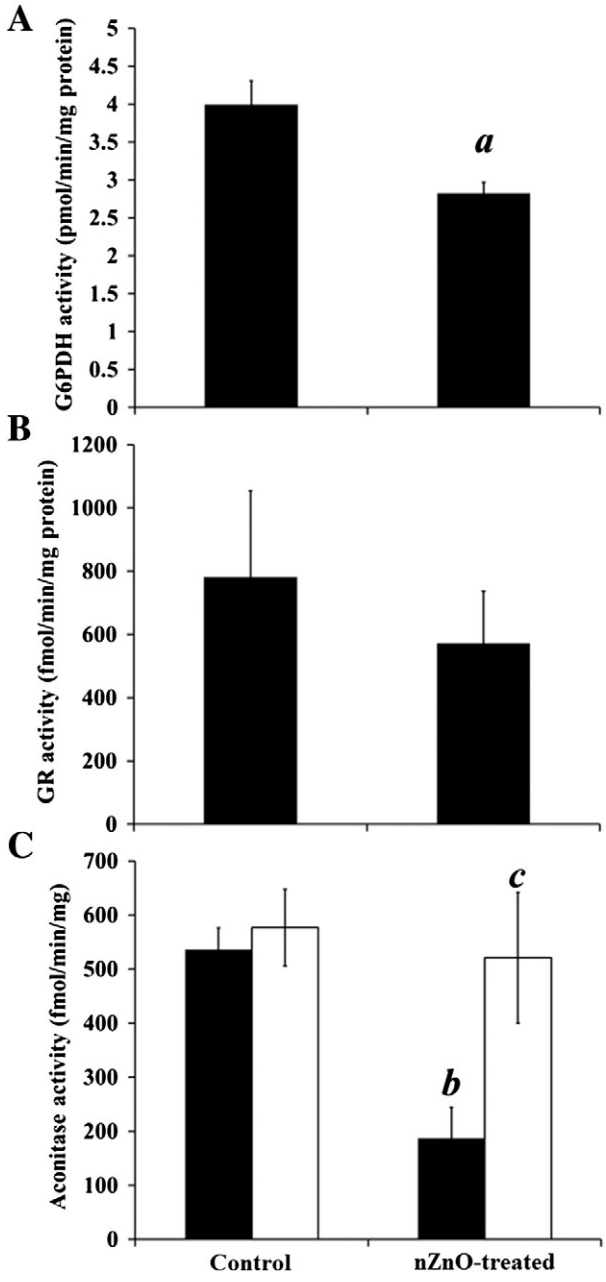

Fig. 2. Effect of fish exposure to nZnO on liver enzyme activity, as determined by colorimetric kinetic enzyme assay. Columns represent means ± SEM. (A) Glucose-6-phosphate dehydrogenase (G6PDH) activity, based on $n = 7$ for both control and nZnO-exposed fish. [a]Indicates a statistically significant difference from control fish as determined by unpaired *t*-test with unequal variances, $p = 0.014$. (B) Glutathione reductase (GR) activity, based on $n = 7$ for both control and nZnO-exposed fish. (C) Aconitase activity. Solid columns (■) represent aconitase activity assayed from $n = 7$ control fish and 6 nZnO-exposed fish, where assays were unsupplemented; empty columns (□) represent aconitase activity assayed from $n = 7$ control fish and 5 nZnO-exposed fish, where assays were supplemented with ferrous ammonium sulfate (Fe^{2+}) to reactivate aconitase that had been inactivated. Effects on results by nZnO exposure, Fe^{2+} supplementation, and potential interaction, were assessed by two-way ANOVA followed by Bonferroni post-tests. Statistically significant differences between specific groups, determined by post-hoc unpaired *t*-test assuming equal variance, were as follows: [b]different from control fish, where aconitase assays were not supplemented with Fe^{2+}, $p < 0.001$; and [c]different from nZnO-exposed fish, where aconitase assays were not supplemented with Fe^{2}, $p = 0.049$.

supernatants (Fig. 3). Total glutathione levels increased by 55.9% as a result of nZnO exposure (Fig. 3A; $n = 5$ control fish and 6 nZnO-exposed fish, $p = 0.031$ by unpaired *t*-test assuming unequal variance). MDA levels, however, appeared not to change (Fig. 3B).

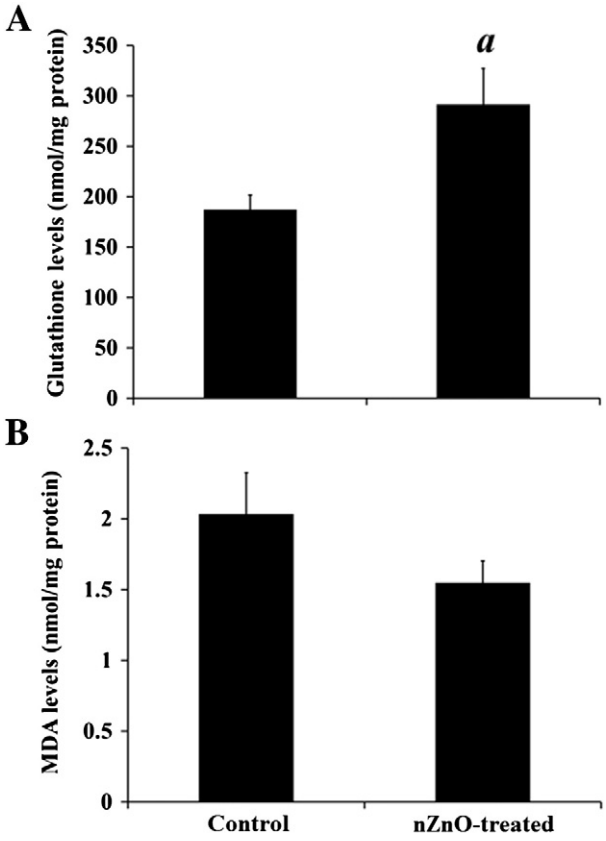

Fig. 3. Effect of fish exposure to nZnO on liver antioxidants and end-products of oxidative stress. Columns represent means ± SEM (A). Total liver glutathione levels, as determined by the colorimetric OxiSelect™ Total Glutathione assay kit. [a]Indicates a statistically significant difference from control fish as determined by unpaired *t*-test assuming unequal variance, based on $n = 5$ control fish and 6 nZnO-exposed fish, $p = 0.031$. (B) MDA levels, as determined by the colorimetric endpoint MDA-586 assay kit, based on $n = 7$ for both control and nZnO-exposed fish.

3.1.3. Validation of assays for liver analytes

It has been previously demonstrated that the results of a multitude of assays may be biased by the presence of ENMs, due to their unique physiochemical properties and their interactions with both the endogenous biomolecules to be assayed, and the assay reagents themselves (Coccini et al., 2010; Ciofani et al., 2010; Boraschi et al., 2011; Wohlleben et al., 2011; MacCormack et al., 2012; Ong et al., 2014). This has potentially led to numerous false positives and false negatives across many nanotoxicology studies. To determine the accuracy of our results, each of the liver assays were validated using liver homogenates that had been partitioned into 3 samples and "spiked" with either MilliQ water, $ZnCl_2$ (to simulate the Zn^{2+} that may be released from nZnO dissolution), or nZnO (Fig. 4). Spiking with Zn^{2+} or nZnO had no statistically significant effect on apparent G6PDH activity or on apparent levels of glutathione (Fig. 4A and E, respectively; as determined by one-way ANOVA), nor any significant effect on apparent aconitase activity (Fig. 4C; as determined by two-way ANOVA followed by post-hoc Bonferroni's test, accounting for treatment, assay supplementation, and interaction). However, one-way ANOVA did show significant differences between groups when assessing GR activity and MDA levels ($p < 0.01$). Post-hoc analyses showed that the presence of 1 mg/L Zn^{2+} significantly affected apparent GR activity and MDA levels. Specifically, Zn^{2+} significantly increased apparent GR activity by 13.5% compared to homogenates spiked with water (Fig. 4B; $n = 3$ assays for liver homogenates spiked with water, $ZnCl_2$, or nZnO, $p = 0.021$ by post-hoc Tukey's multiple comparison test). By contrast, the presence of nZnO did not significantly affect apparent GR activity. Meanwhile,

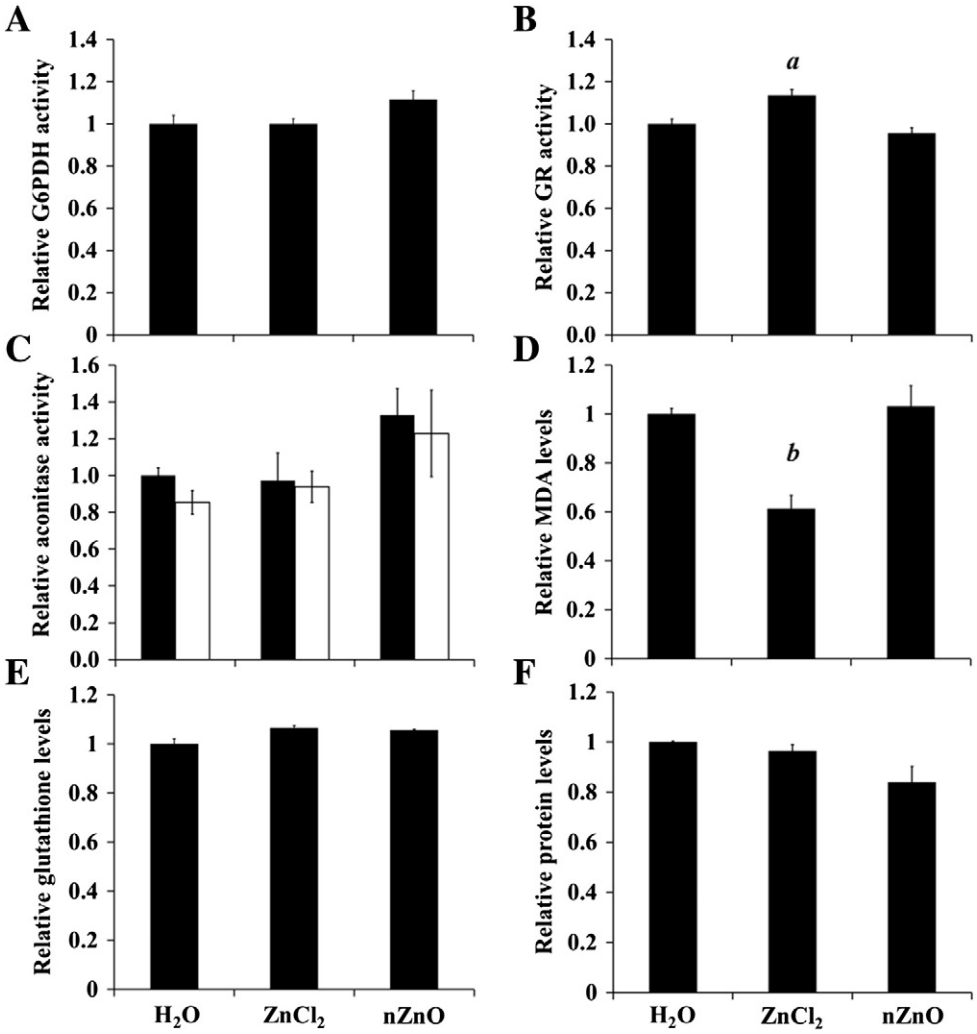

Fig. 4. Validation of assays against interference by Zn^{2+} or nZnO. Columns represent means ± SEM, based on $n = 3$ assays for each of liver homogenate that had been partitioned and "spiked" with MilliQ water (H_2O), 1 mg/L zinc chloride ($ZnCl_2$), or 1 mg/L nZnO (nZnO). (A) Relative detected liver G6PDH activity. (B) Relative detected liver GR activity. (C) Relative detected liver aconitase activity. (D) Relative detected liver MDA levels. (E) Relative detected liver glutathione levels. (F) Relative detected liver protein levels. In the case of validation of aconitase assays, solid columns (■) represent aconitase activity where assays were unsupplemented; empty columns (□) represent aconitase activity where assays were supplemented with ferrous ammonium sulfate (Fe^{2+}). Differences in distribution of data between treatment groups were determined by one-way ANOVA followed by Tukey's post-hoc multiple comparison test. Statistically significant differences between groups were as follows: different from liver homogenates spiked with MilliQ water, $^{a}p = 0.021$ or $^{b}p < 0.01$.

Zn^{2+} significantly and substantially affected apparent MDA levels, decreasing them by 38.6% compared to homogenates spiked with water (Fig. 4D; $n = 3$ assays for liver homogenates spiked with water, $ZnCl_2$, or nZnO, $p < 0.01$ by post-hoc Tukey's multiple comparison test). Again, nZnO did not significantly affect apparent MDA levels. Data for protein levels (Fig. 4F) were found not to be normally distributed by the Shapiro–Wilk test ($p = 0.021$), but no significant differences were found in the distribution of data for protein levels between "spiked" liver treatments by the independent-samples Kruskal–Wallis test.

3.2. Effects of incubation of cell-free rat blood plasma with 1 mg/L nZnO

Control incubations were established for plasma, using saline as a negative control and a final concentration of 1% H_2O_2 as a positive control for oxidative stress. No significant spontaneous oxidative damage was detectable after incubation with supplemented saline for 48 h. 1% H_2O_2, meanwhile, induced oxidative damage rapidly. Interestingly, despite the length of incubations (48 h) and the more favorable thermodynamic conditions (37 °C for rat plasma incubations with nZnO vs. 10 °C for fish exposures to nZnO), no significant nZnO-mediated oxidative damage could be detected in any of the markers assayed.

3.2.1. Plasma MDA and protein carbonyl levels

MDA and protein carbonyl levels were assayed in rat plasma incubated with saline for 48 h, with H_2O_2 (1% final concentration) for 24 h, and with nZnO (1 mg/L final concentration) for 48 h (Fig. 5). No increases in MDA levels were detected in saline-treated plasma after incubation compared to before incubation (Fig. 5A; $n = 8$ saline incubations). H_2O_2 addition resulted in an instantaneous increase in MDA levels, such that a significant, 150% increase was immediately detectable at the "0 h" time-point compared to saline-treated plasma (Fig. 5A; $n = 8$ saline incubations and 3 H_2O_2 incubations, $p < 0.001$ by unpaired t-test assuming unequal variances); these levels rose an additional 80% after 24 h, as compared to H_2O_2-treated plasma before incubation (Fig. 5A; $p < 0.01$ by paired t-test). In nZnO-treated plasma samples, no significant increases were detectable relative to saline-treated plasma (Fig. 5A; $n = 3$ nZnO incubations).

Similarly, no increases in protein carbonyl levels were detected in saline-treated plasma after incubation, compared to before incubation (Fig. 5B; $n = 6$ saline incubations, as determined by nonparametric

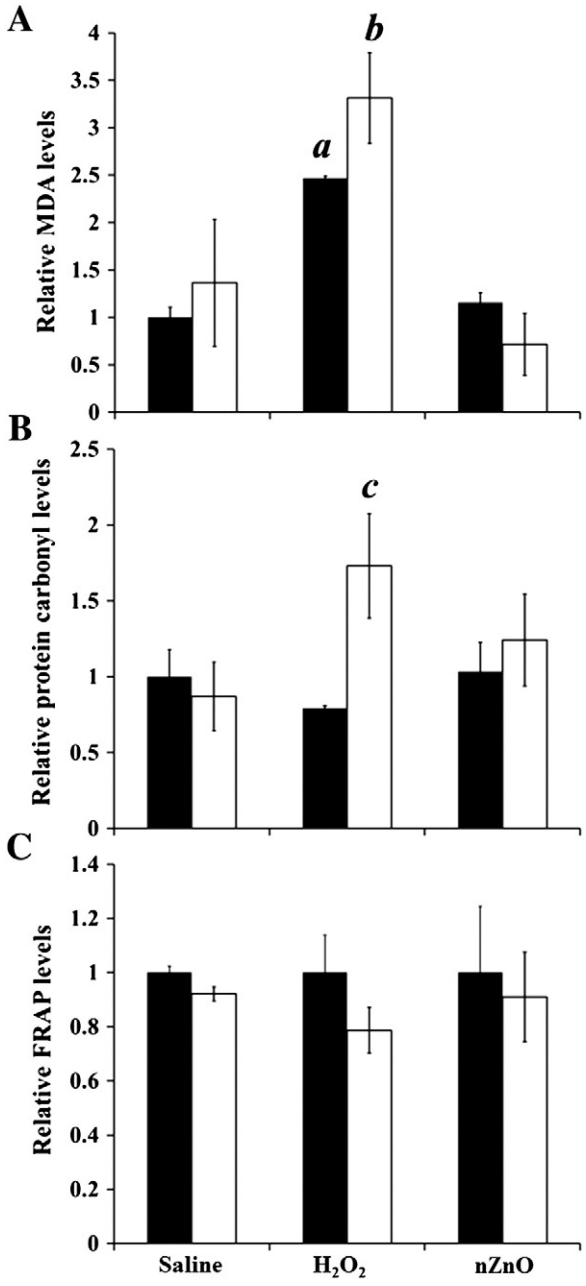

Fig. 5. Effect of cell-free rat blood plasma treatment with nZnO on non-enzymatic markers of oxidative damage, as well as saline (negative control) and H_2O_2 (positive control). (A) Relative plasma MDA levels, as determined by the colorimetric endpoint MDA-586 assay kit. (B) Relative plasma protein carbonyl levels, as determined by colorimetric endpoint assays. (C) Relative FRAP levels, as determined by colorimetric endpoint assays. In each case, columns represent means ± SEM, based on a minimum of $n = 3$ assays (further described in Results) for each treatment and time-point. Solid columns (■) represent biomarker levels before 37 °C incubations (0 h); empty columns (□) represent biomarker levels after 37 °C incubations. Differences between groups caused by both treatment and incubation were assessed as described in detail within the Data analysis section of the Results. Statistically significant differences between groups were as follows: [a]different from saline treatment before incubation, $p < 0.001$ by unpaired *t*-test assuming unequal variance; [b]different from respective treatment before incubation, $p < 0.01$ by paired *t*-test; and [c]different from respective treatment before incubation, $p < 0.01$ by non-parametric Wilcoxon signed-rank tests.

Wilcoxon signed-rank tests). H_2O_2 addition did not result in a rapid reaction as was the case with MDA levels, as protein carbonyl levels did not increase with H_2O_2 treatment at 0 h compared to saline-treated plasma (Fig. 5B; $n = 3$ H_2O_2 incubations, as determined by non-parametric independent-samples Mann–Whitney *U* test). Eventually, H_2O_2 treatment did result in a significant ~119% increase in protein carbonyl levels after incubation (Fig. 5B; $p < 0.01$ by nonparametric Wilcoxon signed-rank tests). Once again, in nZnO-treated plasma samples, no significant increases were detectable, even after incubation, relative to saline-treated plasma (Fig. 5B; $n = 5$ nZnO incubations).

3.2.2. FRAP levels

As with MDA and protein carbonyl levels, FRAP levels were assayed in rat plasma incubated with saline, H_2O_2, or nZnO for 48 h (Fig. 5). No significant decreases in FRAP levels were detected in saline-treated plasma after incubation, compared to before incubation (Fig. 5C; $n = 6$ saline incubations, as determined by nonparametric Wilcoxon signed-rank tests). Incubation with H_2O_2 (positive control) did not result in a significant decrease in FRAP levels compared to H_2O_2-treated plasma before incubation (Fig. 5C; $n = 4$ H_2O_2 incubations, as determined by nonparametric Wilcoxon signed-rank tests). Again, in nZnO-treated plasma samples, no significant decreases in FRAP were detectable, even after incubation, relative to saline-treated plasma (Fig. 5C; $n = 4$ nZnO incubations).

4. Discussion

The toxicity of ENMs to various aquatic organisms is an emerging concern that has garnered much attention over recent years. The molecular and physiological mechanisms of nanotoxicity seem to vary according to the characteristics of the ENM in question and the specific model organism being studied (Handy et al., 2008A; 2008C; MacCormack and Goss, 2008; Johnston et al., 2010; Shaw and Handy, 2011; Schultz et al., 2012). In recent work within our group, we have used a freshwater cypriniform, the white sucker (*Catostomus commersonii*), as our model organism. As a benthic (bottom feeding) fish, it is capable of uptaking both well-dispersed and deposed sedimentary ENMs through dietary and respiratory routes, respectively; previous studies have demonstrated these possible routes of entry in other fish (Handy et al., 2008C; Griffitt et al., 2009; Westerhoff and Nowack, 2012). Our choice of nZnO as a model aquatic nanotoxicant is based on the increasing prevalence of nZnO in a plethora of cosmetics and personal care products; it is perhaps most recognized in everyday usage by its inclusion in sunscreens, alongside TiO_2 nanoparticles (Westerhoff and Nowack, 2012). The latter ENM is increasingly detectable in beach waters (Botta et al., 2011), and thus it is probable that nZnO, too, will soon become equally important as a potential toxicant in aquatic environments.

The present report focuses primarily on liver effects in 14 fish ($n = 7$ for both control and nZnO-exposed fish). Based on the aforementioned studies, we theorized that appreciable nZnO uptake may occur via the gills (and possibly other routes of entry) and cause oxidative stress; it was previously demonstrated that ENMs are capable of translocating across cell membranes (Griffitt et al., 2009; Chou et al., 2011), and thus nZnO may undergo transcytosis across the gill epithelium. Once in the circulatory system, nZnO may be distributed throughout the animal and exert toxicity in other organs or tissues. The present study focused on potential nanotoxic effects in the liver, as it is arguably the most metabolically active and versatile organ in vertebrates.

Three enzymes were assayed in the livers of treated and control fish: 1) G6PDH and GR, commonly known antioxidant enzymes which each contribute to the defense against oxidative stress (Ninfali et al., 1996), and 2) aconitase, an enzymatic biomarker for oxidative damage (Ott et al., 2007). Aconitase showed significant decreases in activity. The catalytic core of aconitase is comprised of an iron–sulfur cluster (4Fe–4S) — however, one of these irons is not coordinated by Cys residues of the protein but rather by water molecules, making it relatively labile. Superoxide accumulation causes a loss of that labile iron, rendering aconitase inactive (Gardner, 2002) and potentially propagating oxidative damage further through the generation of free iron and peroxide (Cantu et al., 2009); reintroduction of supplemental iron can reactivate the enzyme (Gardner et al., 1995; Kruszewski, 2004). Aconitase activity decreased

in white suckers exposed to nZnO, and supplemented iron tended to reactivate it to the original level of activity seen in control fish; this specifically indicates that aconitase activity was reduced due to loss of the labile iron, and not due to decreases in the total protein level or post-translational modification of the enzyme (e.g. phosphorylation; Lin et al., 2009). This is a clear indication that some degree of oxidative stress occurred in the livers of white sucker exposed to nZnO.

The two other enzymes analyzed, G6PDH and GR, are also well known for their roles in antioxidant defense (Pandolfi et al., 1995; Hayes and McLellan, 1999). G6PDH, the first enzyme of the pentose phosphate pathway, is a major source of NADPH in animal cells (Dieni and Storey, 2010; Stanton, 2012). GR directly utilizes this NADPH to reduce GSSG back to GSH, recovering its antioxidant potential (Ninfali et al., 1996; Sies, 1997). At the onset of oxidative stress, both G6PDH and GR activities are expected to be elevated in order to generate sufficient NADPH necessary to rapidly reduce glutathione. However, G6PDH activity instead decreased, and GR activity was unchanged. While this may seem counterintuitive, it is also well-established that levels of antioxidant enzymes may increase, remain unchanged, or even decrease during oxidative stress. In this instance, oxidative species generated by nZnO exposure may have overwhelmed or inhibited antioxidant enzymes (Becker et al., 1998; Préville et al., 1999; Wolf and Baynes, 2007), in a similar vein to the oxidative inactivation of aconitase. If oxidative species do indeed rise to levels high enough to inactivate aconitase and G6PDH, these species can induce dissociation of Nrf2 and Keap1 (Yamamoto et al., 2008; Sekhar et al., 2010), activating transcription of downstream antioxidant defenses (Shih et al., 2003; Lee and Johnson, 2004) including de novo glutathione biosynthesis. This would account for the observation of increased glutathione levels in white sucker livers following nZnO exposure, as well as in other animals, such as rainbow trout following single walled carbon nanotube (SWCNT) exposure (Smith et al., 2007). It would therefore stand to reason that MDA levels would also rise in the face of such accumulating oxidants, however liver MDA levels did not significantly change in white suckers exposed to nZnO. There are, in fact, precedents where MDA levels do not rise in fish during oxidative stress. Lowered levels of lipid peroxidation were seen in rainbow trout exposure to SWCNT (Smith et al., 2007), and in goldfish exposure to iron ions (Bagnyukova et al., 2006), among others. Moreover, lipid peroxidation was unchanged in goldfish livers following exposure to arsenite, despite numerous other markers (superoxide dismutase, catalase, glutathione peroxidase) indicating oxidative stress (Bagnyukova et al., 2007; Lushchak, 2011).

Another major goal of this study was to validate each assay used in our determination of potential nZnO toxicity. Considerable evidence has arisen that ENMs can interfere with numerous assay methods and bias results in both positive and negative directions (Coccini et al., 2010; Ciofani et al., 2010; Boraschi et al., 2011; Wohlleben et al., 2011; MacCormack et al., 2012; Ong et al., 2014). To ensure that our results were not similarly biased and represented the accurate physiological response to nZnO exposure, liver homogenates were partitioned and "spiked" with water and with the same final concentration of nZnO present in exposure tanks, after which they were carried through their normal preparatory and assay steps and compared. An additional validation criterion was the "spiking" of $ZnCl_2$ to the same concentration of nZnO present in exposure tanks; nZnO is known to dissolve in vivo within acidic environments including certain intracellular compartments (Xia et al., 2008; Rasmussen et al., 2010; Cho et al., 2011), and thus it was necessary to ensure that any residual zinc ion in tissues would also not interfere with assay functionality. We found that ionic zinc (from $ZnCl_2$), but not nZnO, interfered with assays for both GR activity and MDA levels. Under the validation conditions tested, Zn^{2+} caused a moderate increase in detected GR activity and a more substantial decrease in detected MDA levels. It is therefore important to note that if there were any appreciable levels of Zn^{2+} present in the liver samples of nZnO-exposed fish, this may have affected the results obtained for GR and MDA. By our assay methods, GR activity and MDA levels did not significantly change in nZnO-exposed white suckers; if any Zn^{2+} present in those liver samples "inflated" GR activity and/or impaired the detection of any physiological rise in MDA levels, then the corrected GR activity and MDA levels in nZnO-exposed fish may ultimately prove significantly lower and higher, respectively, than those observed in control fish. It is difficult to speculate whether nZnO-exposed fish would be expected to accumulate tissue Zn^{2+} at levels similar to the original nZnO exposure; it is noteworthy that the liver does indeed normally function as a central organ in Zn^{2+} homeostasis (Stamoulis et al., 2007), and that oxidative and other physiological stresses can induce the up-regulation of metallothionein and accumulation of Zn^{2+} in liver (Sevcikova et al., 2011; Ruttkay-Nedecky et al., 2013; Tian et al., 2014). A recent study investigating chronic exposure of carp to 0.8 mg/L nZnO revealed extensive histopathological changes to the liver, including the appearance of numerous lysosomes (Lee et al., 2014); this would suggest increased lysosomal nZnO dissolution in livers. Further studies would be needed to explore whether nZnO dissolution in white suckers is in fact significant, and the extent of Zn^{2+} accumulation (if any) in livers.

The question thus raised is the mechanism by which these liver responses are induced, and the potential source of oxidative stress. It was indicated earlier that the unique surface properties of ENMs can directly result in the generation of ROS (Nel et al., 2006; Xia et al., 2008; Rasmussen et al., 2010). However, this was not supported by the conditions of our in vitro incubations of rat blood plasma with 1 mg/L nZnO — the same concentration which provoked numerous hepatic responses in vivo. Despite the interaction of nZnO with a complex biological medium rich in potentially reactive biomolecules, a thermodynamic advantage (from a simple chemical reactivity standpoint, 37 °C vs. 10 °C), and an ample length of time (48 h), we did not detect any oxidative damage in the form of increased MDA levels, increased protein carbonyl levels, or decreased FRAP. A recent in vitro study showed that a number of ENMs (including, fullerenes, nanosilver, nanosilicate, and several others) significantly decrease the ferric reducing ability of serum (FRAS) after only 90 min at 37 °C (Rogers et al., 2008); the concentration of ENMs used in this study, however, was 10 mg/mL or 10,000× the concentration of nZnO in our present study. Similarly, a plethora of inorganic nanoparticles (including Mn_2O_3, Fe_2O_3, Fe^0, ZrO_2, and CeO_2, among many others) were found to reduce L-dopa and generate significant ROS (in the presence of an ROS-sensitive dye, dichlorodihydrofluorescein) in simple phosphate buffer within 30 h at 37 °C (Luna-Velasco et al., 2011); again the concentration of ENMs used in this study was 200 mg/L or 200× the concentration of nZnO in our present study. It would seem, then, that while very elevated concentrations of EMNs can generate oxidative damage in vitro, at lower concentrations (e.g. 1 mg/L nZnO), stress indicators are only observed in the presence of intracellular components, and/or a living, responsive unit (from a single cell, upwards); simple biochemical reactivity between relatively low concentrations of nZnO and a complex mixture of biomolecules is insufficient to mimic the response observed in live fish.

The physiological responses to nZnO seen in this study may be the result of an immune system response. The size of ENMs, and the characteristics of the protein coronae they assemble (including antibodies and complement proteins), make them prime targets for phagocytosis by immune cells, particularly by Kupffer cells in the liver (Sadauskas et al., 2007; Aggarwal et al., 2009; Nie, 2010; Jennifer and Maciej, 2013). The respiratory burst used by macrophages (such as Kupffer cells) to destroy microbes or particles will generate a number of reactive species including $O_2^{\bullet-}$, H_2O_2, and nitric oxide ($\cdot NO$), among others. Kupffer cells have long been implicated in liver toxicity (Rusyn et al., 1999), and have now resurged as a prominent mechanism for ENM-mediated hepatic injury (Chen et al., 2013). At present, however, these mechanisms are highly speculative, and warrant further studies in order to confirm them.

Overall, the present work has shown that exposure of a benthic fish to relatively low levels of commercially-relevant ENMs can induce a detectable stress-response in liver tissue. We have also demonstrated that the breakdown products of ENMs (in this case, ionic zinc) can affect the validity of assays used to detect common biomarkers of oxidative stress. Moreover, we have shown that with these low concentrations of ENMs, biomarkers will only show stress indicators in living, responsive units, and not through in vitro exposure with non-responsive biological media, regardless of the complexity of that media. Had we relied solely on in vitro methods to screen for oxidative stress potential (e.g. Rogers et al., 2008), in this situation/at this ENM concentration, nZnO would have resulted in a false negative. These results illustrate that ENMs do pose risks to aquatic organisms, emphasizing a clear need for further research into their mechanism(s) of toxicity. Our results also illustrate the need to assess the broader downstream consequences of the enzyme changes seen here, such as the effects on hepatic Krebs' cycle as a result of aconitase inhibition. Finally, once again, we also highlight the need for rigorous and meticulous validation of all methodology used in nanotoxicity testing in order to ensure accurate conclusions.

Acknowledgments

We would like to thank Mr. Wayne Anderson and the Harold Crabtree Aqualab at Mount Allison University for assistance with collection and care of experimental animals. We also thank Mr. James Ehrman at the Mount Allison University Digital Microscopy Facility for assistance with scanning electron microscopy imaging. We additionally thank Dr. Terry Belke and Ms. Jackie Jacob-Vogels for their assistance and their gift of rat blood that allowed us to optimize our initial plasma experiments prior to using commercial preparations. Finally, we thank Ms. Maria Thistle for her invaluable assistance in helping us perfect our statistical analyses. This research was funded by a Margaret and Wallace McCain Postdoctoral Fellowship to CAD, a Goodridge Summer Research Scholarship to NIC, and a Universitas Summer Undergraduate Award to KMAB. TJM was supported by a Natural Sciences and Engineering Research Council of Canada Discovery Grant and a New Brunswick Health Research Foundation Operating grant. The authors declare no conflict of interest in the work presented here.

References

Aggarwal, P., Hall, J.B., McLeland, C.B., Dobrovolskaia, M.A., McNeilm, S.E., 2009. Nanoparticle interaction with plasma proteins as it relates to particle distribution, biocompatibility, and therapeutic efficacy. Adv. Drug Deliv. Rev. 61, 428–437.

Aitken, R.J., Chaudhry, M.Q., Boxall, A.B..A., Hull, M., 2006. Manufacture and use of nanomaterials: current use in the UK and global trends. Occup. Med. 56, 300–306.

Bagnyukova, T.V., Chahrak, O.I., Lushchak, V.I., 2006. Coordinated response of goldfish antioxidant defenses to environmental stress. Aquat. Toxicol. 78, 325–331.

Bagnyukova, T.V., Luzhna, L.I., Pogribny, I.P., Lushchak, V.I., 2007. Oxidative stress and antioxidant defenses in goldfish liver in response to short-term exposure to arsenite. Environ. Mol. Mutagen. 48, 658–665.

Bai, W., Zhang, Z., Tian, W., He, X., Ma, Y., Zhao, Y., Chai, Z., 2010. Toxicity of zinc oxide nanoparticles to zebrafish embryo: a physicochemical study of toxicity mechanism. J. Nanopart. Res. 12, 1645–1654.

Becker, K., Savvides, S.N., Keese, M., Schirmer, R.H., Karplus, P.A., 1998. Enzyme inactivation through sulfhydryl oxidation by physiologic NO-carriers. Nat. Struct. Biol. 5, 267–271.

Boraschi, D., Oostingh, G.J., Casals, E., Italiani, P., Nelissen, I., Puntes, V.F., Duschl, A., 2011. Nano-immunosafety: issues in assay validation. J. Phys. Conf. Ser. 304, 012077.

Botta, C., Labille, J., Auffan, M., Borschneck, D., Miche, H., Cabié, M., Masion, A., Rose, J., Bottero, J.Y., 2011. TiO_2-based nanoparticles released in water from commercialized sunscreens in a life-cycle perspective: Structures and quantities. Environ. Pollut. 159, 1543–1550.

Cantu, D., Schaack, J., Patel, M., 2009. Oxidative inactivation of mitochondrial aconitase results in iron and H_2O_2-mediated neurotoxicity in rat primary mesencephalic cultures. PLoS ONE 4, e7095.

Cedervall, T., Hansson, L.A., Lard, M., Frohm, B., Linse, S., 2012. Food chain transport of nanoparticles affects behavior and fat metabolism in fish. PLoS ONE 7, e32254.

Chen, Q., Xue, Y., Sun, J., 2013. Kupffer cell-mediated hepatic injury by silica nanoparticles *in vitro* and *in vivo*. Int. J. Nanomedicine 8, 1129–1140.

Cho, W.S., Duffin, R., Howie, S.E.M., Scotton, C.J., Wallace, W.A.H., MacNee, W., Bradley, M., Megson, I.L., Donaldson, K., 2011. Progressive severe lung injury by zinc oxide nanoparticles; the role of Zn^{2+} dissolution inside lysosomes. Part. Fibre Toxicol. 8, 27.

Chou, L.Y.T., Ming, K., Chan, W.C.W., 2011. Strategies for the intracellular delivery of nanoparticles. Chem. Soc. Rev. 40, 233–245.

Ciofani, G., Danti, S., D'Alessandro, D., Moscato, S., Menciassi, A., 2010. Assessing cytotoxicity of boron nitride nanotubes: interference with the MTT assay. Biochem. Biophys. Res. Commun. 394, 405–411.

Coccini, T., Roda, E., Sarigiannis, D.A., Mustarelli, P., Quartarone, E., Profumo, A., Manzo, L., 2010. Effects of water-soluble functionalized multi-walled carbon nanotubes examined by different cytotoxicity methods in human astrocyte D384 and lung A549 cells. Toxicology 269, 41–53.

Dieni, C.A., Storey, K.B., 2010. Regulation of glucose-6-phosphate dehydrogenase by reversible phosphorylation in liver of a freeze tolerant frog. J. Comp. Physiol. B 180, 1133–1142.

Dieni, C.A., Stone, C.J.L., Armstrong, M.L., Callaghan, N.I., MacCormack, T.J., 2013. Spherical gold nanoparticles impede the function of bovine serum albumin *in vitro*: a new consideration for studies in nanotoxicology. J. Nanomater. Mol. Nanotechnol. 2, 6.

Finkel, T., Holbrook, N.J., 2000. Oxidants, oxidative stress and the biology of ageing. Nature 408, 239–247.

Gardner, P.R., 2002. Aconitase: sensitive target and measure of superoxide. Methods Enzymol. 349, 9–23.

Gardner, P.R., Raineri, I., Epstein, L.B., White, C.W., 1995. Superoxide radical and iron modulate aconitase activity in mammalian cells. J. Biol. Chem. 270, 13399–13405.

Griffitt, R.J., Hyndman, K., Denslow, N.D., Barber, D.S., 2009. Comparison of molecular and histological changes in zebrafish gills exposed to metallic nanoparticles. Toxicol. Sci. 107, 404–415.

Guo, D., Bi, H., Liu, B., Wu, Q., Wang, D., Cui, Y., 2013. Reactive oxygen species-induced cytotoxic effects of zinc oxide nanoparticles in rat retinal ganglion cells. Toxicol. In Vitro 27, 731–738.

Handy, R.D., Henry, T.B., Scown, T.M., Johnston, B.D., Tyler, C.R., 2008a. Manufactured nanoparticles: their uptake and effects on fish — a mechanistic analysis. Ecotoxicology 17, 396–409.

Handy, R.D., Owen, R., Valsami-Jones, E., 2008b. The ecotoxicology of nanoparticles and nanomaterials: current status, knowledge, gaps, challenges, and future needs. Ecotoxicology 17, 315–325.

Handy, R.D., von der Kammer, F., Lead, J.R., Hassellöv, M., Owen, R., Crane, M., 2008c. The ecotoxicology and chemistry of manufactured nanoparticles. Ecotoxicology 17, 287–314.

Handy, R.D., Cornelis, G., Fernandes, T., Tsyusko, O., Decho, A., Sabo-Atwood, T., Metcalf, C., Steevens, J.A., Klaine, S.J., Koelmans, A.A., et al., 2012. Ecotoxicity test methods for engineered nanomaterials: practical experiences and recommendations from the bench. Environ. Toxicol. Chem. 31, 15–31.

Hayes, J.D., McLellan, L.I., 1999. Glutathione and glutathione-dependent enzymes represent a co-ordinately regulated defence against oxidative stress. Free Radic. Res. 31, 273–300.

Jennifer, M., Maciej, W., 2013. Nanoparticle technology as a double-edged sword: cytotoxic, genotoxic, and epigenetic effects on living cells. J. Nanomater. Bionanotechnol. 4, 53–63.

Johnston, B.D., Scown, T.M., Moger, J., Cumberland, S.A., Baalousha, M., Linge, K., van Aerle, R., Jarvis, K., Lead, J.R., Tyler, C.R., 2010. Bioavailability of nanoscale metal oxides TiO_2, CeO_2, and ZnO to fish. Environ. Sci. Technol. 44, 1144–1151.

Kruszewski, M., 2004. Labile iron pool: the main determinant of cellular response to oxidative stress. Mutat. Res. 531, 81–92.

Lee, J.M., Johnson, J.A., 2004. An important role of Nrf2-ARE pathway in the cellular defense mechanism. J. Biochem. Mol. Biol. 37, 139–143.

Lee, J.W., Kim, J.E., Shin, Y.J., Ryu, J.S., Eom, I.C., Lee, J.S., Kim, Y., Kim, P.J., Choi, K.H., Lee, B.C., 2014. Serum and ultrastructure responses of common carp (*Cyprinus carpio* L.) during long-term exposure to zinc oxide nanoparticles. Ecotoxicol. Environ. Saf. 104, 9–17.

Lin, G., Brownsey, R.W., MacLeod, K.M., 2009. Regulation of mitochondrial aconitase by phosphorylation in diabetic rat heart. Cell. Mol. Life Sci. 66, 919–932.

Luna-Velasco, A., Field, J.A., Cobo-Curiel, A., Sierra-Alvarez, R., 2011. Inorganic nanoparticles enhance the production of reactive oxygen species (ROS) during the autoxidation of L-3,4-dihydroxyphenylalanine (L-dopa). Chemosphere 85, 19–25.

Lushchak, V.I., 2011. Environmentally induced oxidative stress in aquatic animals. Aquat. Toxicol. 101, 13–30.

Lynch, I., Dawson, K.A., 2008. Protein–nanoparticle interactions. Nano Today 3, 40–47.

MacCormack, T.J., Goss, G.G., 2008. Identifying and predicting biological risks associated with manufactured nanoparticles in aquatic ecosystems. J. Ind. Ecol. 12, 286–296.

MacCormack, T.J., Clark, R.J., Dang, M.K.M., Ma, G., Kelly, J.A., Veinot, J.G.C., Goss, G.G., 2012. Inhibition of enzyme activity by nanomaterials: potential mechanisms and implications for nanotoxicity testing. Nanotoxicology 6, 514–525.

Mu, L., Sprando, R.L., 2010. Application of nanotechnology in cosmetics. Pharm. Res. 27, 1746–1749.

Nel, A., Xia, T., Mädler, L., Li, N., 2006. Toxic potential of materials at the nanolevel. Science 311, 622–627.

Nie, S., 2010. Understanding and overcoming major barriers in cancer nanomedicine. Nanomedicine 5, 523–528.

Ninfali, P., Cuppini, C., Marinoni, S., 1996. Glucose-6-phosphate dehydrogenase and glutathione reductase support antioxidant enzymes in nerves and muscles of rats during nerve regeneration. Restor. Neurol. Neurosci. 10, 69–75.

Ong, K.J., MacCormack, T.J., Clark, R.J., Ede, J.D., Ortega, V.A., Felix, L.C., Dang, M.K.M., Ma, G., Fenniri, H., Veinot, J.G.C., Goss, G.G., 2014. Widespread nanoparticle-assay interference: implications for nanotoxicity testing. PLoS ONE 9, e90650.

Ott, M., Gogvadze, V., Orrenius, S., Zhivotovsky, B., 2007. Mitochondria, oxidative stress and cell death. Apoptosis 12, 913–922.

Pandolfi, P.P., Sonati, F., Rivi, R., Mason, P., Grosveld, F., Luzzatto, L., 1995. Targeted disruption of the housekeeping gene encoding glucose 6-phosphate dehydrogenase

(G6PD): G6PD is dispensable for pentose synthesis but essential for defense against oxidative stress. EMBO J. 14, 5209–5215.
Park, J.Y., Ramachandran, G., Raynor, P.C., Kim, S.W., 2011. Estimation of surface area concentration of workplace incidental nanoparticles based on number and mass concentrations. J. Nanopart. Res. 13, 4897–4911.
Préville, X., Salvemini, F., Giraud, S., Chaufour, S., Paul, C., Stepien, G., Ursini, M.V., Arrigo, A.P., 1999. Mammalian small stress proteins protect against oxidative stress through their ability to increase glucose-6-phosphate dehydrogenase activity and by maintaining optimal cellular detoxifying machinery. Exp. Cell Res. 247, 61–78.
Prousek, J., 2007. Fenton chemistry in biology and medicine. Pure Appl. Chem. 79, 2325–2338.
Rahman, M., Laurent, S., Tawil, N., L'Hocine, Y., Mahmoudi, M., 2013. Nanoparticle and protein corona. Protein–nanoparticle interactions: The bio–nano interface. Springer-Verlag Heidelberg, pp. 21–44.
Rasmussen, J.W., Martinez, E., Louka, P., Wingett, D.G., 2010. Zinc oxide nanoparticles for selective destruction of tumor cells and potential for drug delivery applications. Expert Opin. Drug Deliv. 7, 1063–1077.
Rogers, E.J., Hsieh, S.F., Organti, N., Schmidt, D., Bello, D., 2008. A high throughput *in vitro* analytical approach to screen for oxidative stress potential exerted by nanomaterials using a biologically relevant matrix: human blood serum. Toxicol. In Vitro 22, 1639–1647.
Rusyn, I., Bradham, C.A., Cohn, L., Schoonhoven, R., Swenberg, J.A., Thurman, R.D., 1999. Corn oil rapidly activates nuclear factor-κB in hepatic Kupffer cells by oxidant-dependent mechanisms. Carcinogenesis 20, 2095–2100.
Ruttkay-Nedecky, B., Nejdl, L., Gumulec, J., Zitka, O., Masarik, M., Eckschlager, T., Stiborova, M., Adam, V., Kizek, R., 2013. The role of metallothionein in oxidative stress. Int. J. Mol. Sci. 14, 6044–6066.
Sadauskas, E., Wallin, H., Stoltenberg, M., Vogel, U., Doering, P., Larsen, A., Danscher, G., 2007. Kupffer cells are central in the removal of nanoparticles from the organism. Part. Fibre Toxicol. 4, 10.
Schultz, A.G., Ong, K.J., MacCormack, T.J., Ma, G., Veinot, J.G.C., Goss, G.G., 2012. Silver nanoparticles inhibit sodium uptake in juvenile rainbow trout (*Oncorhynchus mykiss*). Environ. Sci. Technol. 46, 10295–10301.
Sekhar, R.M., Rachakonda, G., Freeman, M.L., 2010. Cysteine-based regulation of the CUL3 adaptor protein Keap1. Toxicol. Appl. Pharmacol. 241, 21–26.
Sevcikova, M., Modra, H., Slaninova, A., Svobodova, Z., 2011. Metals as a cause of oxidative stress in fish: a review. Vet. Med. Czech 56, 537–546.
Shaw, B.J., Handy, R.D., 2011. Physiological effects of nanoparticles on fish: a comparison of nanometals versus metal ions. Environ. Int. 37, 1083–1097.
Shih, A.Y., Johnson, D.A., Wong, G., Kraft, A.D., Jiang, L., Erb, H., Johnson, J.A., Murphy, T.H., 2003. Coordinate regulation of glutathione biosynthesis and release by Nrf2-expressing glia potently protects neurons from oxidative stress. J. Neurosci. 23, 3394–3406.
Sies, H., 1997. Oxidative stress: oxidants and antioxidants. Exp. Physiol. 82, 291–295.
Smith, C.J., Shaw, B.J., Handy, R.D., 2007. Toxicity of single walled carbon nanotubes to rainbow trout, (*Oncorhynchus mykiss*): respiratory toxicity, organ pathologies, and other physiological effects. Aquat. Toxicol. 82, 94–109.
Stamoulis, I., Kouraklis, G., Theocharis, S., 2007. Zinc and the liver: an active interaction. Dig. Dis. Sci. 52, 1595–1612.
Stanton, R.C., 2012. Glucose-6-phosphate dehydrogenase, NADPH, and cell survival. IUBMB Life 64, 362–369.
Tian, X., Zheng, Y., Li, Y., Shen, Z., Tao, L., Dou, X., Qian, J., Shen, H., 2014. Physiological stress induced accumulation and up-regulation of ZIP14 and metallothionein in rat liver. BMC Gastroenterol. 14, 32.
Umrani, R.D., Paknikar, K.M., 2014. Zinc oxide nanoparticles show antidiabetic activity in streptozotocin-induced types-1 and 2 diabetic rats. Nanomedicine 9, 89–104.
Wang, J., 2005. Carbon-nanotube based electrochemical sensors: a review. Electroanalysis 17, 7–14.
Westerhoff, P., Nowack, B., 2012. Searching for global descriptors of nanomaterial fate and transport in the environment. Acc. Chem. Res. 46, 844–853.
Wohlleben, W., Kolle, S.N., Hasenkamp, L.C., Böser, A., Vogel, S., von Vacano, B., van Ravenzwaay, B., Landsiedel, R., 2011. Artifacts by marker enzyme adsorption on nanomaterials in cytotoxicity assays with tissue cultures. J. Phys. Conf. Ser. 304, 012061.
Wolf, M.B., Baynes, J.W., 2007. Cadmium and mercury cause an oxidative stress-induced endothelial dysfunction. Biometals 20, 73–81.
Xia, T., Kovochich, M., Liong, M., Mädler, L., Gilbert, B., Shi, H., Yeh, J.I., Zinc, J.I., Nel, A.E., 2008. Comparison of the mechanism of toxicity of zinc oxide and cerium oxide nanoparticles based on dissolution and oxidative stress properties. ACS Nano 2, 2121–2134.
Yamamoto, T., Suzuki, T., Kobayashi, A., Wakabayashi, J., Maher, J., Motohashi, H., Yamamoto, M., 2008. Physiological significance of reactive cysteine residues of Keap1 in determining Nrf2 activity. Mol. Cell. Biol. 28, 2758–2770.